Modeling and Measurement of the Influence of Antenna Transversal Location on Tunnel Propagation

Chenming Zhou and Ronald Jacksha
National Institute for Occupational Safety and Health
Pittsburgh, PA, USA, 15237
{czhou, rjacksha}@cdc.gov

***Abstract*—The ray tracing and modal methods are applied to model the influence of antenna location (within the tunnel cross section) on tunnel propagation. Measurement results in a railroad tunnel are provided to validate the models. Simulation results are shown to agree with measurement results well. Both simulation and measurement results suggest that more receive power can be obtained by placing the transmitter or receiver antenna close to the center location of the tunnel cross section.**

I. Introduction

Radio propagation in tunnels has been extensively investigated recently. Most of the studies in the literature, however, focus on propagation analysis in the longitudinal dimension. In this paper, we investigate the power distribution in the cross section of the tunnel and study the influence of antenna location within the cross section on tunnel propagation.

II. Modeling

We consider a straight rectangular tunnel with a width of 2a and a height of 2b. The coordinate system is orientated in the center of the tunnel, with x horizontal, y vertical, and z down the tunnel. Within the tunnel, a transmitter is located at T(x0, y0, 0) and a receiver at R(x, y, z). Without loss of generality, we also assume the source is vertically polarized.

A. Ray tracing method

Based on the ray tracing theory, the received electric field can be obtained by summing the scalar electric fields of the rays from all the images of the point source as [1]:

$$E_r(x,y,z) = E_t \sum_{m=-\infty}^{+\infty} \sum_{n=-\infty}^{+\infty} \frac{e^{-jkr_{m,n}}}{r_{m,n}} \rho_\perp^{|m|} \rho_{//}^{|n|} \tag{1}$$

where

$$r_{m,n} = \sqrt{(2ma+(-1)^m x_0 - x)^2 + (2nb+(-1)^n y_0 - y)^2 + z^2} \tag{2}$$

$$\rho_\perp = \frac{\cos\theta_\perp - \sqrt{\bar{\varepsilon}_a - 1 + \cos^2\theta_\perp}}{\cos\theta_\perp + \sqrt{\bar{\varepsilon}_a - 1 + \cos^2\theta_\perp}}$$
$$\rho_{//} = \frac{\cos\theta_{//} - \sqrt{\bar{\varepsilon}_b - 1 + \cos^2\theta_{//}}/\bar{\varepsilon}_b}{\cos\theta_{//} + \sqrt{\bar{\varepsilon}_b - 1 + \cos^2\theta_{//}}/\bar{\varepsilon}_b} \tag{3}$$

$$\cos\theta_\perp = \frac{|2ma + (-1)^m x_0 - x|}{r_{m,n}}$$
$$\cos\theta_{//} = \frac{|2nb + (-1)^n y_0 - y|}{r_{m,n}} \tag{4}$$

In (1), E_t is the magnitude of the transmitted electric field, k is the wave number in the waveguide (free space). In (3), $\bar{\varepsilon}_{a,b} = \left[\varepsilon_{a,b} - j\sigma_{a,b}/(2\pi f)\right]/\varepsilon_0$ are the complex relative permittivities of the vertical and horizontal walls , respectively. Here f is the frequency, and $\varepsilon_{a,b}$ and $\sigma_{a,b}$ are the permittivities and conductivities of the corresponding tunnel walls. The magnetic permeability of all media are assumed to be the same and equal to permeability of the free space μ_0.

B. Modal method

As shown in [1], the electric field at an arbitrary position within a dielectric rectangular tunnel can also be viewed as the superposition of the electric fields from different hybrid modes ($EH_{p,q}$) :

$$E_r = \frac{-j2\pi E_t}{ab} \sum_{p=1}^{+\infty}\sum_{q=1}^{+\infty} A_{p,q} \frac{e^{-(\alpha_{p,q}+j\beta_{p,q})z}}{\beta_{p,q}} \tag{5}$$

where

$$A_{p,q} = \sin\left(\frac{p\pi}{2a}x + \varphi_p\right)\sin\left(\frac{q\pi}{2b}y + \varphi_q\right)$$
$$\sin\left(\frac{p\pi}{2a}x_0 + \varphi_p\right)\sin\left(\frac{q\pi}{2b}y_0 + \varphi_q\right) \tag{6}$$

$$\varphi_{p,q} = \begin{cases} 0 & \text{p(q) is even} \\ \pi/2 & \text{p(q) is odd} \end{cases} \tag{7}$$

$$\beta_{p,q} = \sqrt{k^2 - \left(\frac{p\pi}{2a}\right)^2 - \left(\frac{q\pi}{2b}\right)^2} \tag{8}$$

$$\alpha_{p,q} = \frac{1}{b}\left(\frac{q\lambda}{4b}\right)^2 \frac{\bar{\varepsilon}_b}{\sqrt{\bar{\varepsilon}_b - 1}} + \frac{1}{a}\left(\frac{p\lambda}{4a}\right)^2 \frac{1}{\sqrt{\bar{\varepsilon}_a - 1}} \tag{9}$$

III. Measurement

Propagation measurements were conducted in a vacated railroad tunnel with its cross-section view shown in Fig. 2 (a). The tunnel is rectangular with an arched roof. The maximum height of the tunnel is 6.7 m and the width of the tunnel is 4.9 m. The length of the tunnel is about 800 m. The walls and ceiling are smooth with some rough sections due to deterioration of the concrete. The rails and ties have been removed leaving only the crushed stone track ballast. For all the tests reported in the paper, the transmitter and receiver were set to a height of 2.14 m.

The RF test apparatus was comprised of two components: a stationary RF transmitter and a mobile RF receiver (shown in Fig 1 (b)). The transmitter consisted of an RF signal source connected to a transmit antenna (Tx). The receiver (Rx) consisted of an RF spectrum analyzer connected through an RF A/B switch to either a 50 Ω termination or a receive antenna.

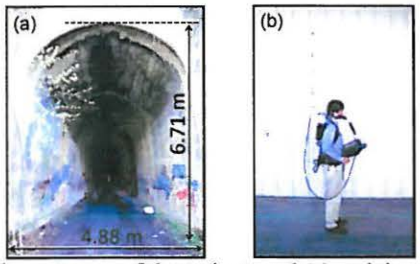

Fig. 1. The entrance of the train tunnel (a) and the receiver used for the propagation measurements (b).

IV. Results and Discussion

Fig. 2 shows a comparison of measured power attenuations at 455 MHz with Tx and Rx placed at different locations within the tunnel cross section. The first and second letters in the legend denote the Tx and Rx locations, respectively, with "C' for center, "L" left, and "R" right. For example, the curve labeled "CR" was measured by placing the transmitter in the center and moving the receiver along the right side of the tunnel. For all the measurements reported in this paper, the transmitted power is always fixed. It is found from Fig. 2 that the power decay at far distances for different combinations of the Tx/Rx locations are similar to each other, with the exception of fixed power offsets. The maximum receive power occurs when both Tx and Rx are placed in the center. Moving either Tx or Rx away from the center location leads to a decrease of received power. Similar measurement observations are also reported in [2] in a road tunnel.

Fig. 3 shows the corresponding simulated power attenuations based on the ray tracing and modal methods introduced in Section II, respectively. The measured tunnel has an arched ceiling but its cross session has been approximated by an equivalent rectangle of the same width (4.9 m) and a height of 6.6 m for modeling purposes. The same electrical properties ($\mathrm{Re}\{\bar{\varepsilon}_{a,b}\}=7$ and $\sigma_{a,b}=0.05$ S/m) are used for all four tunnel walls and all four frequencies. It is shown that both ray tracing and modal methods give consistent results for different Tx/Rx locations. A comparison of Fig. 2 to Fig. 3 shows that simulation results match the measurement results well, indicating that both the ray tracing and modal methods are accurate for modeling the influence of antenna location on tunnel propagation.

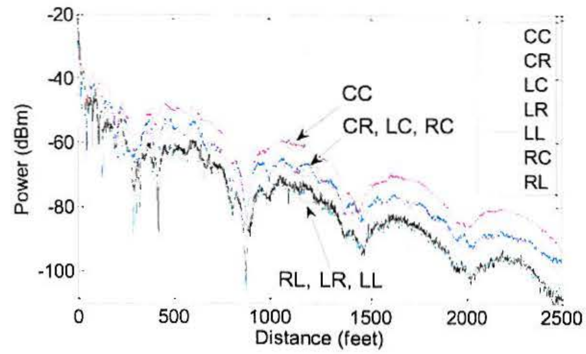

Fig. 2. A comparison of measured power decays with Tx/Rx placed at different locations within the tunnel cross section.

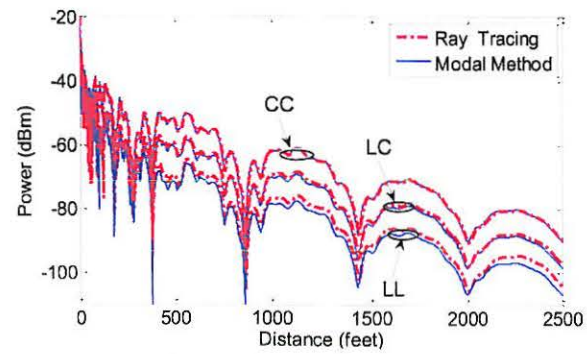

Fig. 3. A comparison of simulated power decays with Tx/Rx placed at different locations within the tunnel cross section.

V. Conclusion

RF measurements are conducted in an abandoned railroad tunnel with Tx and Rx antennas placed at different locations within the cross section. Ray tracing and modal methods are shown to be accurate for modeling the influence of antenna location on tunnel propagation. Both the simulated and measured results show that more receive power can be obtained by placing either the Tx or Rx close to the center location within a tunnel cross section. Therefore, it is suggested that antennas of underground wireless communication and tracking systems should be mounted close to the center location and away from the four walls when possible for a better radio coverage.

Acknowledgement

We would like to thank Mr. Timothy Plass for his help on taking the measurement data. We also thank Dr. Joseph Waynert for many useful discussions.

References

[1] C. Zhou and J. Waynert, "The Equivalence of the Ray Tracing and Modal Methods for Modeling Radio Propagation in Lossy Rectangular Tunnels," IEEE Antennas and Wireless Propagation Letters, vol. 13, pp. 615-618, 2014.

[2] M. Lienard, A. Nasr, J. G. Pardo, and P. Degauque, "Experimental analysis of wave depolarization in arched tunnels,". IEEE 18th International Symposium on Personal, Indoor and Mobile Radio Communications, (PIMRC), pp. 1-4, Sept 3-7, 2007